

See discussions, stats, and author profiles for this publication at: <https://www.researchgate.net/publication/231705860>

# Tuning the Phase Behavior of Polystyrene-block-poly(n-alkyl methacrylate) Copolymers by Introducing Random Copolymer for Methacrylate Block

ARTICLE *in* MACROMOLECULES · JULY 2009

Impact Factor: 5.8 · DOI: 10.1021/ma9007016

---

CITATIONS

10

---

READS

13

3 AUTHORS, INCLUDING:



Sung Hyun Han

Samsung Advanced Institute of Technology

15 PUBLICATIONS 185 CITATIONS

SEE PROFILE

# Tuning the Phase Behavior of Polystyrene-*block*-poly(*n*-alkyl methacrylate) Copolymers by Introducing Random Copolymer for Methacrylate Block

Hong Chul Moon, Sung Hyun Han, and Jin Kon Kim\*

National Creative Research Initiative Center for Block Copolymer Self-Assembly, Department of Chemical Engineering, Pohang University of Science and Technology, Pohang, Kyungbuk 790-784, Republic of Korea

Junhan Cho\*

Department of Polymer Science and Engineering and Center for Photofunctional Energy Materials, Dankook University, 126 Jukjeon-dong, Yongin-si, Gyeonggi-do 448-701, Korea

Received April 1, 2009; Revised Manuscript Received June 1, 2009

## 1. Introduction

Block copolymers have gained increasing interest because of their self-assembly into periodic morphologies such as lamellae, hexagonally packed cylinders, spheres (body-centered cubic), and gyroids with nanometer length scale.<sup>1–5</sup> The phase behavior of a block copolymer depends on the volume fraction (*f*) of one of the blocks, the degree of polymerization (*N*), and the Flory–Huggins segmental interaction parameter ( $\chi$ ).<sup>1</sup> Among many block copolymers, weakly interacting polystyrene-*block*-poly(*n*-alkyl methacrylate) copolymers (PS-*b*-PnAMA) show various phase behaviors depending on the length of alkyl chain in PnAMA: order-to-disorder transition (ODT),<sup>6–8</sup> lower disorder-to-order transition (LDOT),<sup>7–9</sup> and a closed-loop (immiscibility loop) with both LDOT and upper order-to-disorder transition (UODT) upon heating.<sup>7,10–15</sup> The phase behavior of PS-*b*-PnAMA was successfully explained by a compressible random phase approximation developed by us.<sup>7,15,24,25</sup>

Very recently, we found closed-loop phase behavior for polystyrene-*block*-poly(*n*-butyl-*ran*-*n*-hexyl)methacrylate copolymers (PS-*b*-Pn(B-*r*-H)MA)<sup>15</sup> similar to polystyrene-*block*-poly(*n*-pentyl methacrylate) copolymers (PS-*b*-PnPMA),<sup>10</sup> whereas PS-*b*-PnHMA showed only ODT-type phase behavior, but PS-*b*-PnBMA exhibited LDOT-type phase behavior.<sup>7–9</sup> Also, the pressure coefficient of the transition temperatures for PS-*b*-Pn(B-*r*-H)MA ( $dT_{LDOT}/dP = +595$  °C/kbar and  $dT_{UODT}/dP = -700$  °C/kbar)<sup>15</sup> was much greater than that of PS-*b*-PnBMA ( $dT_{LDOT}/dP = +147$  °C/kbar)<sup>20</sup> and PS-*b*-PnHMA ( $dT_{UODT}/dP = -60$  °C/kbar).<sup>19</sup> Since the carbon numbers in the alkyl group of PnBMA and PnHMA are 4 and 6, respectively, the random copolymer, Pn(B-*r*-H)MA, consisting of the same molar ratio of PnBMA and PnHMA, would exhibit a similar phase behavior to PnPMA with *n* = 5. Namely, an average force field of Pn(B-*r*-H)MA having the same weight fraction of PnBMA and PnHMA would be similar to that of PnPMA.

Ruzette et al. reported that polystyrene-*block*-poly(methacrylate-*ran*-lauryl methacrylate) copolymers (PS-*b*-P(MMA-*r*-LMA)) exhibited the LDOT, even though both PS-*b*-PMMA and PS-*b*-PLMA exhibited the ODT.<sup>6–8</sup> They explained this interesting phase behavior by the fact that the specific volume and the solubility parameter of P(MMA-*r*-LMA) are very similar to

those of neat PnBMA,<sup>8</sup> which exhibited the LDOT. They also found that the  $dT/dP$  of the LDOT of PS-*b*-P(MMA-*r*-LMA) was 150 °C/kbar,<sup>19</sup> which is similar to that (147 °C/kbar) of PS-*b*-PnBMA.<sup>20</sup>

Thus, it is interesting to investigate whether the closed-loop phase behavior is observed for polystyrene-*block*-poly(*n*-alkyl-*ran*-*n'*-alkyl methacrylate) copolymers with very different values of *n* and *n'*. To prove this postulation, we chose polystyrene-*block*-poly(*n*-octyl-*ran*-methyl) methacrylate copolymers (PS-*b*-Pn(O-*r*-M)MA) (namely, *n* = 8 and *n'* = 1). We found that when the total molecular weight and the composition of the random copolymer block were judiciously controlled, PS-*b*-Pn(O-*r*-M)MA exhibited closed-loop phase behavior having both LDOT and UODT within an experimentally accessible temperature range. This is an interesting result because both PS-*b*-PMMA and PS-*b*-PnOMA showed only ODT during heating.<sup>6–8</sup> This is distinctly in contrast to PS-*b*-Pn(B-*r*-H)MA where PS-*b*-PnBMA showed LDOT, whereas PS-*b*-PnOMA exhibited UODT. We consider that the closed-loop phase behavior observed for PS-*b*-Pn(O-*r*-M)MA is attributed to the fact that the average force field of Pn(O-*r*-M)MA with ~70/30 (w/w) PnOMA/PMMA composition would be similar to that of PnPMA. Furthermore, PS-*b*-PMMA exhibited small barotropicity with  $dT_{ODT}/dP = +23$  °C/kbar<sup>7,19</sup> (that is, the miscibility between PS and PMMA decreases with increasing *P*), while PS-*b*-PnOMA showed very weak baroplasticity with  $dT_{ODT}/dP = -5$  °C/kbar<sup>19</sup> (that is, the miscibility between two block components is slightly enhanced upon pressurization). However, PS-*b*-Pn(O-*r*-M)MA showed excellent baroplasticity similar to PS-*b*-PnPMA<sup>18</sup> and PS-*b*-Pn(B-*r*-H)MA.<sup>15</sup> We explained this phase behavior by using a compressible random phase approximation.

## 2. Experimental Section

Symmetric PS-*b*-Pn(O-*r*-M)MAs with various molecular weights were synthesized by sequential anionic polymerization of styrene and the monomer mixture composed of MMA and *n*-OMA (30/70 w/w) in dried tetrahydrofuran (THF) at -78 °C under a purified argon atmosphere with *sec*-butyllithium (*sec*-BuLi) as an initiator and dried LiCl as an additive to prepare narrow molecular weight distribution for methacrylate moiety.<sup>21</sup> The dibutylmagnesium was used to purify styrene monomer, and the trioctylaluminum was used to purify MMA and *n*-OMA. After the polymerization of styrene for 1 h, a mixture of MMA

\*To whom correspondence should be addressed. E-mail: jkkim@postech.ac.kr (J.K.K.); jhcho@dankook.ac.kr (J.C.).

Table 1. Molecular Characteristics of Polymers Employed in This Study

sample code	$M_n$	$M_w/M_n$	$w_{PS}$	PS- <i>b</i> -Pn(O- <i>r</i> -M)MA-L/PS- <i>b</i> -Pn(O- <i>r</i> -M)MA-H (w/w)	wt % of POMA/PMMA in the Pn(O- <i>r</i> -M)MA
PS- <i>b</i> -Pn(O- <i>r</i> -M)MA-L	51 000	1.06	0.506	100/0	66/34
PS- <i>b</i> -Pn(O- <i>r</i> -M)MA-B1	52 900 <sup>a</sup>			53/47	
PS- <i>b</i> -Pn(O- <i>r</i> -M)MA-B2	53 050 <sup>a</sup>			50/50	
PS- <i>b</i> -Pn(O- <i>r</i> -M)MA-B3	53 200 <sup>a</sup>			47/53	
PS- <i>b</i> -Pn(O- <i>r</i> -M)MA-H	55 300	1.05	0.49	0/100	68/32

<sup>a</sup> Calculated by  $(M_n)_{blend} = [(w_1/M_{n,1}) + (w_2/M_{n,2})]^{-1}$ , where  $w_i$  and  $M_{n,i}$  are weight fraction and number-average molecular weight of polymer  $i$ , respectively.

and *n*-OMA was added dropwise into the reactor and reacted for 5 h. We also synthesized anionically the random copolymer of Pn(O-*r*-M)MA at various reaction times to check the randomness of the two components. The synthesized PS-*b*-Pn(O-*r*-M)MA and Pn(O-*r*-M)MA were characterized by size exclusion chromatography (SEC: Waters) with PS standards in tetrahydrofuran (THF) solution and <sup>1</sup>H nuclear magnetic resonance spectroscopy (NMR: Bruker DPX300) and are summarized in Table 1. Since the transition temperatures of PS-*b*-Pn(O-*r*-M)MA are very sensitive to a small difference in the total molecular weight, the molecular weight was carefully controlled by blending of PS-*b*-Pn(O-*r*-M)MA-H and PS-*b*-Pn(O-*r*-M)MA-L with methylene chloride as a solvent and slowly evaporating solvent for 24 h at room temperature. All samples were annealed at 140 °C for 48 h under vacuum.

An Advanced Rheometric Expansion System (TI Instrument) with parallel plates of 25 mm diameter was used to perform the dynamic temperature sweep of the storage and loss moduli ( $G'$  and  $G''$ ) under isochronal conditions upon heating at a rate of 0.5 °C/min. The angular frequency and the strain amplitude were 0.1 rad/s and 0.05, respectively, which lie in the linear viscoelasticity range.

Depolarized transmitted light scattering<sup>22</sup> was used to determine the transition temperatures (LDOT and UODT) of PS-*b*-Pn(O-*r*-M)MAs at various hydrostatic pressures. Vertically polarized light from a HeNe laser with a wavelength of 632.8 nm passed through the sample with pressure cell designed by us and a horizontal analyzing polarizer onto a photodetector. Sample thickness was 1.0 mm, and the heating rate was 1 °C/min.

SAXS experiments were performed on beamlines 4C1 and 4C2 at the Pohang Light Source (Korea), where a W/B4C double multilayer delivered monochromatic X-rays on the samples with a wavelength of 0.1608 nm.<sup>23</sup> The sample-to-detector distance was 2 m. A 2-D CCD camera (Princeton Instruments, SCX-TE/CCD-1242) was used to collect the scattered X-rays. The sample thickness and the exposure time were 2.0 mm and 300 s, respectively. SAXS profiles were obtained upon heating at a rate of 0.5 °C/min. We found that thermal degradation did not occur during rheology and SAXS experiments, as confirmed by SEC and <sup>1</sup>H NMR.

### 3. Results and Discussion

Because of the large difference in alkyl chain length in PMMA ( $n' = 1$ ) and PnOMA ( $n = 8$ ), the randomness of Pn(O-*r*-M)MA block should be checked. For this purpose, we analyzed several Pn(O-*r*-M)MA aliquots corresponding to different polymerization times (1 min to 5 h) by using SEC and <sup>1</sup>H NMR. Figure 1a gives NMR spectra for the Pn(O-*r*-M)MA samples prepared at different polymerization times. It is seen that the change in the weight fraction of MMA and *n*-OMA in all the samples obtained from the peak ratio at position *a* (MMA) and *b* (*n*-OMA) was very small (less than 2%), even though the number-average molecular weight ( $M_n$ ) was changed greatly from 10 000 to 136 000 (see Figure S1 and Table S1 in the Supporting Information). These results indicate that the synthesized Pn(O-*r*-M)MA block is regarded as a random copolymer, not a tapered (gradient) or block copolymer.

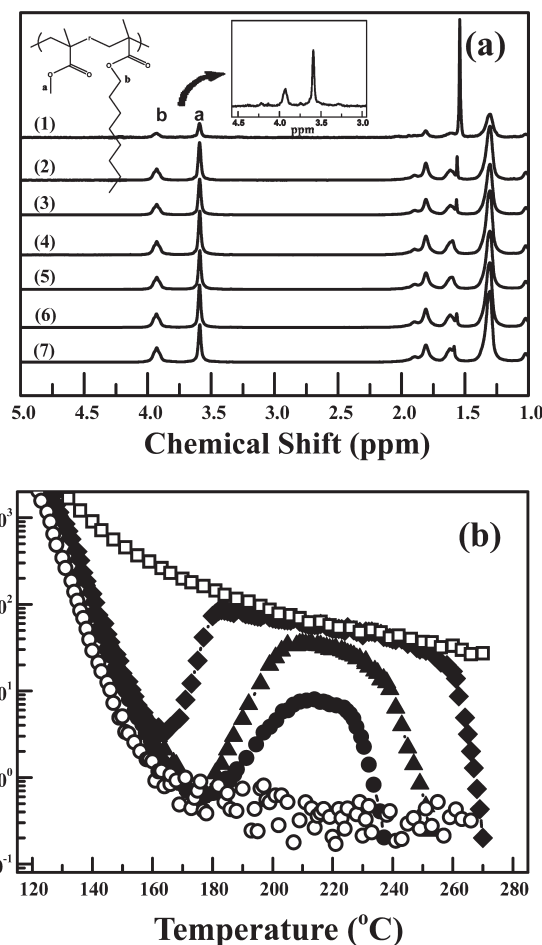


**Figure 1.** (a) <sup>1</sup>H NMR spectra of Pn(O-*r*-M)MA aliquots at various polymerization times (min): (1) 1, (2) 3, (3) 6, (4) 12, (5) 22, (6) 31, and (7) 70. The <sup>1</sup>H NMR spectra at reaction times of 2 and 5 h are essentially the same as those at 70 min. The inset is the enlarged <sup>1</sup>H NMR spectrum corresponding to 1 min. (b) Temperature dependence of  $G'$  at  $\omega = 0.1$  rad/s obtained during heating at a rate of 0.5 °C/min for PS-*b*-Pn(O-*r*-M)MA-L (○), PS-*b*-Pn(O-*r*-M)MA-H (□), PS-*b*-Pn(O-*r*-M)MA-B1 (●), PS-*b*-Pn(O-*r*-M)MA-B2 (▲), and PS-*b*-Pn(O-*r*-M)MA-B3 (◆).

To support this argument, we also synthesized anionically two homopolymers of PMMA and PnOMA and measured their glass transition temperatures ( $T_g$ ) of these two and Pn(O-*r*-M)MA. A single  $T_g$  for Pn(O-*r*-M)MA was observed between  $T_g$  of two homopolymers (see Figure S1b in the Supporting Information). However, one might raise the question that even though the synthesized Pn(O-*r*-M)MA is tapered (or block) copolymer, a single  $T_g$  could be observed when the molecular weight of Pn(O-*r*-M)MA is small and becomes disordered state. To exclude this possibility, we carried out turbidity experiment for the mixture of 70/30 (w/w) PnOMA with  $M_n = 3200$  and PMMA with  $M_n = 1500$ . The macrophase-separated morphology was observed even at 220 °C (see Figure S1c), which suggests poor miscibility between PMMA and PnOMA. On the other hand, the

synthesized Pn(O-*r*-M)MA has a molecular weight of 138 000 and a weight fraction of PnOMA having 0.65; thus, the molecular weight of PnOMA and PMMA in the Pn(O-*r*-M)MA is  $\sim 30$  times larger than that of PnOMA and PMMA used in the turbidity experiment. Therefore, if the synthesized Pn(O-*r*-M)MA had been tapered (or block) copolymer, it should have exhibited the microphase-separated morphology, resulting in two  $T_g$ s corresponding to PnOMA and PMMA blocks. But, it showed a single  $T_g$ , as shown in Figure S1b; the turbidity experiment confirms again that the synthesized Pn(O-*r*-M)MA is not a block (or tapered) copolymer but a random copolymer.

Figure 1b gives temporal changes of storage modulus  $G'$  of neat PS-*b*-Pn(O-*r*-M)MA-L, PS-*b*-Pn(O-*r*-M)MA-H, and three mixtures of these two neat block copolymers. Although the total molecular weight difference of two neat PS-*b*-Pn(O-*r*-M)MAs was very small (less than 10%), the phase behavior was completely different. Namely, PS-*b*-Pn(O-*r*-M)MA-L with lower molecular weight showed fully disordered over the entire experimental temperature range, whereas PS-*b*-Pn(O-*r*-M)MA-H with slightly higher molecular weight became fully ordered. But, when these two block copolymers were properly mixed, the closed-loop phase behavior was observed. Interestingly, even when the total molecular weight difference was very small (less than  $\sim 0.5\%$ ) from PS-*b*-Pn(O-*r*-M)MA-B1 to PS-*b*-Pn(O-*r*-M)MA-B3, the closed-loop size changed remarkably. It is noted that the polydispersity of the three blended samples was at most 1.057, very similar to that of neat PS-*b*-Pn(O-*r*-M)MA-L because of similar  $M_n$  ( $\sim 8\%$ ) of two neat block copolymers. Therefore, the transition temperatures of the blended samples are very close to those of the corresponding neat block copolymers at a given total molecular weight.

Figure 2a gives SAXS profiles of PS-*b*-Pn(O-*r*-M)MA-B2 at various temperatures. Because of small electron density difference between PS and Pn(O-*r*-M)MA, high order peaks were not observed. Only a weak and broad correlation hole peak was observed at lower temperatures. As temperature increased above LDOT, the SAXS peak became sharp. Even though higher order peaks were not detected, this sharp peak should not be considered as the peak arising from the correlation hole effect in the disordered state. This is because of large values of  $G'$  (see Figure 1b) and the nonzero birefringence (see Figure S2 in the Supporting Information) at temperatures where a sharp SAXS peak was observed. When the temperature was increased further, this sharp peak became broad at UODT. Plots of the inverse of the maximum intensity ( $1/I(q_{\max})$ ) and the full width at half-maximum (fwhm) versus the inverse of the absolute temperature ( $1/T$ ) for PS-*b*-Pn(O-*r*-M)MA-B2 and PS-*b*-Pn(O-*r*-M)MA-B3 are shown in parts b and c of Figure 2, respectively. Both LDOT and UODT of PS-*b*-Pn(O-*r*-M)MA copolymers were observed within the experimental temperature range, and the values are consistent with those of the rheological method.

Two transition temperatures of these three blended copolymers are plotted with  $M_n$  in Figure 3a. When we extrapolated these data, PS-*b*-Pn(O-*r*-M)MA would become fully disordered state for  $M_n < 52\,750$ . This value is slightly larger than that 47 200 for PS-*b*-PnMA<sup>10</sup> and 48 100 PS-*b*-Pn(B-*r*-H)MA.<sup>15</sup> Figure 3b gives the dependence of LDOT and UODT for PS-*b*-Pn(O-*r*-M)MA-B2 on hydrostatic pressure measured by birefringence.  $dT_{\text{LDOT}}/dP$  and  $dT_{\text{UODT}}/dP$  of PS-*b*-Pn(O-*r*-M)MA-B2 were  $+590$  °C/kbar and  $-750$  °C/kbar, respectively, at pressures above 30 bar. Very interestingly, even though PS-*b*-PMMA showed barotropicity ( $dT_{\text{ODT}}/dP = +23$  °C/kbar)<sup>7,19</sup> and PS-*b*-PnOMA showed very weak baroplasticity ( $dT_{\text{ODT}}/dP = -5$  °C/kbar),<sup>19</sup> PS-*b*-Pn(O-*r*-M)MA showed very strong baroplasticity similar to PS-*b*-PnMA<sup>18</sup> and PS-*b*-Pn(B-*r*-H)MA.<sup>15</sup>

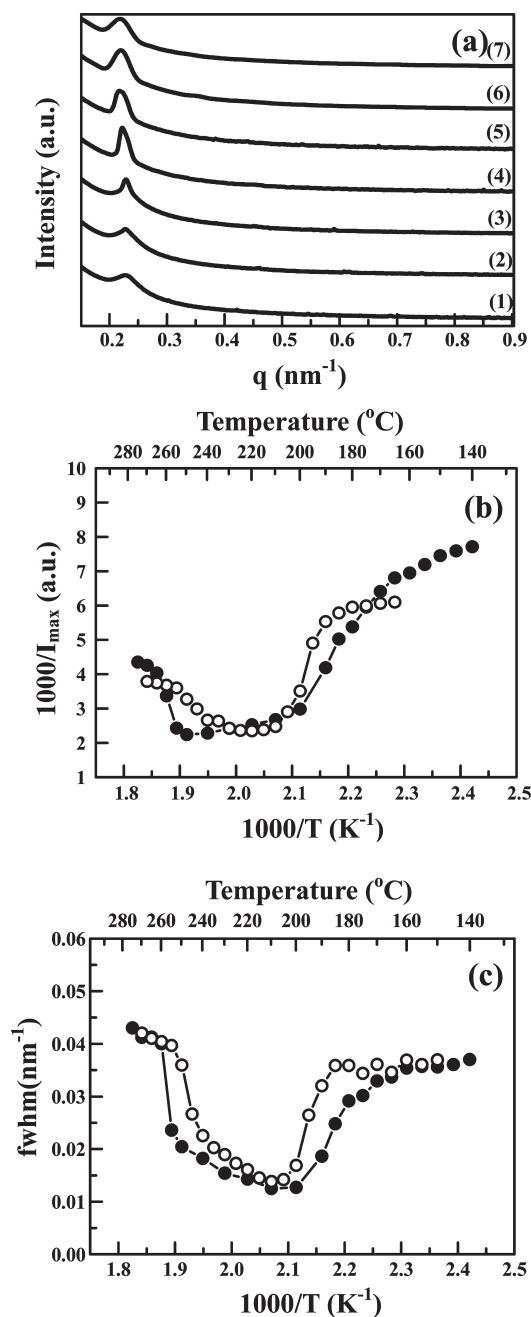


**Figure 2.** (a) SAXS profiles of PS-*b*-Pn(O-*r*-M)MA-B2 at various temperatures obtained during heating at a rate of 0.5 °C/min: (1) 190, (2) 195, (3) 200, (4) 225, (5) 245, (6) 250, and (7) 255 °C. Plots of the inverse of the maximum intensity ( $1/I(q_{\max})$ ) (b) and the full width at half-maximum (fwhm) (c) versus the inverse of the absolute temperature ( $1/T$ ) for PS-*b*-Pn(O-*r*-M)MA-B2 (○) and PS-*b*-Pn(O-*r*-M)MA-B3 (●).

In our previous studies on PS-*b*-poly(*n*-alkyl methacrylates) (PS-*b*-PnAMA) systems, the LDOT or closed-loop type behavior of PS-*b*-PnAMA with ethyl ( $n = 2$ ) to pentyl ( $n = 5$ ) side group was attributed to the existence of the directional interaction (DI), resulting from the dipole/induced dipole interaction from the phenyl ring in PS and the polar ester group of PnAMA.<sup>16,17</sup> On the other hand, the rigidity of the methyl side group for PS-*b*-poly(methyl methacrylate) (PS-*b*-PMMA) and the great flexibility of bulky side groups with large excluded volume for PS-*b*-PnAMA having *n*-hexyl or larger groups ( $n \geq 6$ ) hinder these block copolymers from forming the favorable DI, which leads to exhibiting only ODT-type phase behavior.<sup>6–8</sup>



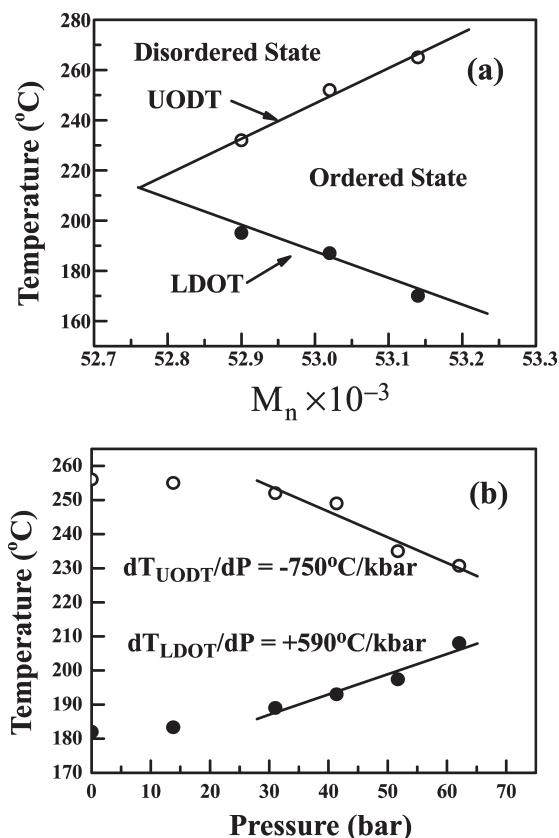


**Figure 3.** (a) Dependence of LDOT (●) and UODT (○) on  $M_n$ . (b) Changes of LDOT (●) and UODT (○) for PS-*b*-Pn(O-*r*-M)MA-B2 with hydrostatic pressure measured by birefringence.

To explain the closed-loop phase behavior observed for PS-*b*-Pn(O-*r*-M)MA, even though both PS-*b*-PMMA ( $n=1$ ) and PS-*b*-PnOMA ( $n=8$ ) showed only ODT-type phase behavior, we consider the effective Flory interaction parameter  $\chi_F$ , which can be divided into two terms:  $\chi_{\text{app}}$  for exchange energy and  $\chi_{\text{comp}}$  for compressibility difference. A few equation-of-state parameters are needed to evaluate  $\chi_F$ .<sup>24,25</sup> These are self-interaction  $\varepsilon_{11}/k$  and  $\varepsilon_{22}/k$ , theoretical monomer diameter  $\sigma_i$ , and a composite parameter  $(N\pi\sigma^3/6M)_i$  representing the  $N/M$  ratio for each block  $i$ . Here, the symbols  $k$ ,  $N$ , and  $M$  denote the Boltzmann constant, chain size, and molecular weight, respectively. The cross-interaction,  $\varepsilon_{12}$ , is taken around the Berthelot's rule  $(\varepsilon_{11}\varepsilon_{22})^{1/2}$ , and  $\sigma$  and  $(N\pi\sigma^3/6M)$  for mixtures adopt a Lorentz-type rule  $(X_1 + X_2)/2$ . The detailed theoretical explanations are given in the Supporting Information.

According to the theoretical results, when one block is replaced by a random copolymer consisting of PMMA and PnOMA, the excluded volume per one unit can be tuned to be similar to that of PnPMA. Also, the large flexibility of the *n*-octyl group in the random copolymer block is significantly reduced in the average sense because of the random participation of the rigid PMMA into flexible PnOMA. Therefore, the average force field (and  $\Delta\varepsilon \equiv \varepsilon_{11} + \varepsilon_{22} - 2\varepsilon_{12}$ ) generated by the Pn(O-*r*-M)MA block becomes similar to that by the PnPMA block. As a result, DI between Pn(O-*r*-M)MA block and phenyl rings in PS block would be possible, which results in the closed-loop phase behavior. In addition,  $\varepsilon_{\text{Pn(O-r-M)MA}}$  having similar value of  $\varepsilon_{\text{PnPMA}}$  yields the composition ( $\phi$ ) dependence of pressure,  $\partial P/\partial\phi$  (or  $\chi_{\text{comp}}$ ), for a block copolymer large enough to have strong baroplasticity.

Following a Hartree (fluctuation correction) analysis based on a compressible random phase approximation (RPA),<sup>26,27</sup> symmetric diblock copolymers reach their ODT, if  $N\chi_F$  evaluated at a

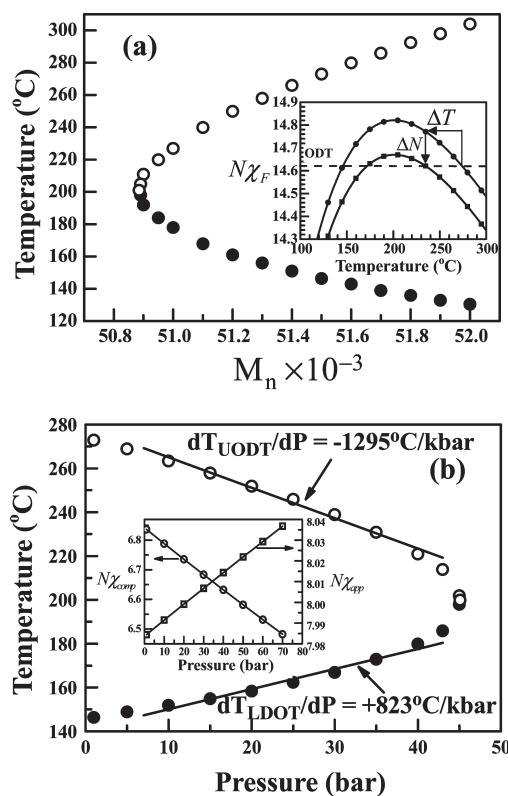


**Figure 4.** Plots of the theoretically predicted (a) LDOT (●) and UODT (○) versus  $M_n$ . The inset gives plots of  $N\chi_F$  versus temperature for symmetric PS-*b*-Pn(O-*r*-M)MA with two different  $M_n$ s ( $M_n = 51\,500$  (●) and  $M_n = 50\,974$  (■)). The dashed line in the inset indicates  $N\chi_F$  value at ODT. (b) Dependence of LDOT (●) and UODT (○) for PS-*b*-Pn(O-*r*-M)MA ( $M_n = 51\,500$ ) on hydrostatic pressure. The inset gives plots of  $N\chi_{\text{app}}$  and  $N\chi_{\text{comp}}$  versus  $P$  at 200 °C.

wavenumber characterizing microphases becomes  $10.495 + 41.022 N^{-1/3}$  no matter how they respond to pressure (baroplastic or barotropic). The value of  $N\chi_{F,\text{ODT}}$  for the symmetric PS-*b*-Pn(O-*r*-M)MA with  $M_n = 51\,500$  ( $N=980$ ) is predicted to be 14.62. Since Pn(O-*r*-M)MA yields a force field similar to PnPMA, the cross-interaction  $\varepsilon_{ij}$  ( $= 0.983(\varepsilon_{\text{PS}}\varepsilon_{\text{Pn(O-r-M)MA}})^{1/2}$ ) and its increment  $\delta\varepsilon$  ( $= 0.185 \varepsilon_{\text{PS}}$ ) due to the formation of DI for PS-*b*-Pn(O-*r*-M)MA adopts those for PS-*b*-PnPMA.<sup>26</sup> The presence of DI in PS-*b*-Pn(O-*r*-M)MA yields a maximum of  $N\chi_F$  when it is plotted against temperature. As the chain size decreases,  $N\chi_F$  decreases by  $\Delta N\chi_F$ . The new LDOT and UODT upon the decrease of  $N$  should be changed by  $\Delta T$ , as schematically shown in the inset of Figure 4a. Around the maximum of  $N\chi_F$ , its slope approaches zero. In this situation, only a slight change in  $N\chi_F$  makes enormous changes in  $\Delta T$ .<sup>15</sup> Such a strong molecular weight dependence of the predicted LDOT and UODT in the closed loop is indeed shown in Figure 4a. Interestingly, the predicted loops depending on  $M_n$  are similar to the experimentally determined ones, even though there is no adjustable parameter in estimating the block copolymer phase behavior.

In Figure 4b, the changes of LDOT and UODT are shown as a function of pressure for PS-*b*-Pn(O-*r*-M)MA of  $M_n = 51\,500$ . The dependence of  $\chi_{\text{app}}$  and  $\chi_{\text{comp}}$  on pressure is different, as shown in the inset of Figure 4b.<sup>26,28</sup> If  $\Delta\varepsilon > 0$ , the  $\chi_{\text{app}}$  increases upon pressurization because of the increased contact density. On the contrary, the applied pressure reduces  $\chi_{\text{comp}}$  to enhance miscibility because the increased bulk modulus ( $B_T$ ) of the block copolymer suppresses the compressibility difference effect. We found that  $N\chi_F$  for PS-*b*-Pn(O-*r*-M)MA is reduced upon pressurization because  $N\chi_{\text{comp}}$  changes more rapidly than  $N\chi_{\text{app}}$ . When  $P$  is  $\sim 45$  bar,  $N\chi_F$  becomes smaller than the  $N\chi_{F,\text{ODT}}$ ,

indicating that the closed loop disappears. Although the predicted pressure coefficients of UODT and LDOT for PS-*b*-Pn(O-*r*-M)MA are somewhat larger than those measured experimentally, these are again noteworthy because the prediction was done without using any adjustable parameters. The large pressure coefficients were again attributed to the fact that around the maximum of the  $N\chi_F$  a slight reduction in  $N\chi_F$  due to pressure makes enormous changes in  $\Delta T$ .

While the above experimental observations are well explained by the molecular model based on the compressible RPA, it would be interesting to predict the closed-loop phase behavior in PS-*b*-Pn(O-*r*-M)MA by using other molecular approaches such as the lattice cluster theory<sup>29–32</sup> whose ordering mechanism is totally different from ours.

#### 4. Conclusions

We have shown that symmetric PS-*b*-Pn(O-*r*-M)MA copolymers exhibited closed-loop phase behavior with very large pressure coefficients, even though PS-*b*-PMMA and PS-*b*-PnOMA showed only ODT-type phase behavior as well as barotropicity (PS-*b*-PMMA) and very weak baroplasticity (PS-*b*-PnOMA). Furthermore, we have shown that the concept of the average force field generated by Pn(O-*r*-M)MA yields an environment similar to that of PnPMA. Therefore, the observed closed-loop phase behavior of PS-*b*-Pn(O-*r*-M)MA can be attributed to the finely tuned directional interaction between the phenyl ring of PS and the ester groups of Pn(O-*r*-M)MA.

**Acknowledgment.** This work was supported by the National Creative Research Initiative Program supported by the Korean Organization of Science and Engineering Foundation (KOSEF). Small-angle X-ray scattering was performed at PLS beamline supported by POSCO and KOSEF. J.C. acknowledges the financial support from the GRRC Program of Gyeonggi province (GRRCdankook2009-B04).

**Supporting Information Available:** SEC and DSC results for verifying randomness of the random copolymer, Pn(O-*r*-M)MA; OM image for the 70/30 (w/w) PnOMA/PMMA; temperature dependence of birefringence for PS-*b*-Pn(O-*r*-M)MA-B2; detailed explanations of the employed theory and calculation of the transition temperatures for PS-*b*-Pn(O-*r*-M)MA. This material is available free of charge via the Internet at <http://pubs.acs.org>.

#### References and Notes

(1) Leibler, L. *Macromolecules* **1980**, *13*, 1602.

- (2) Bates, F. S.; Fredrickson, G. H. *Annu. Rev. Phys. Chem.* **1990**, *41*, 525.
- (3) Kim, J. K.; Lee, J. I.; Lee, D. H. *Macromol. Res.* **2008**, *16*, 267.
- (4) Hashimoto, T. In *Thermoplastic Elastomers*; Legge, N. R., Holden, G., Schroeder, H. E., Eds.; Hanser: New York, 1987.
- (5) Hamley, I. W. *The Physics of Block Copolymers*; Oxford University Press: New York, 1998.
- (6) Zhao, Y.; Sivaniah, E.; Hashimoto, T. *Macromolecules* **2008**, *41*, 9948.
- (7) Ryu, D. Y.; Shin, C.; Cho, J.; Lee, D. H.; Kim, J. K.; Lavery, K. A.; Russell, T. P. *Macromolecules* **2007**, *40*, 7644.
- (8) Ruzette, A.-V. G.; Banerjee, P.; Mayes, A. M.; Pollard, M.; Russell, T. P.; Jerome, R.; Slawacki, T.; Hjelm, R.; Thiagarajan, P. *Macromolecules* **1998**, *31*, 8509.
- (9) Russell, T. P.; Karis, T. E.; Gallot, Y.; Mayes, A. M. *Nature (London)* **1994**, *368*, 729.
- (10) Ryu, D. Y.; Jeong, U.; Kim, J. K.; Russell, T. P. *Nat. Mater.* **2002**, *1*, 114.
- (11) Ryu, D. Y.; Park, M. S.; Chae, S. H.; Jang, J.; Kim, J. K.; Russell, T. P. *Macromolecules* **2002**, *35*, 8676.
- (12) Ryu, D. Y.; Jeong, U.; Lee, D. H.; Kim, J.; Youn, H. S.; Kim, J. K. *Macromolecules* **2003**, *36*, 2894.
- (13) Ryu, D. Y.; Lee, D. H.; Jeong, U.; Yun, S. H.; Park, S.; Kwon, K.; Sohn, B. H.; Chang, T.; Kim, J. K.; Russell, T. P. *Macromolecules* **2004**, *37*, 3717.
- (14) Ruzette, A.-V. G. *Nat. Mater.* **2002**, *1*, 85.
- (15) Moon, H. C.; Han, S. H.; Kim, J. K.; Li, G. H.; Cho, J. *Macromolecules* **2008**, *41*, 6793.
- (16) Kim, H. J.; Kim, S. B.; Kim, J. K.; Jung, Y. M.; Ryu, D. Y.; Lavery, K. A.; Russell, T. P. *Macromolecules* **2006**, *39*, 408.
- (17) Kim, H. J.; Kim, S. B.; Kim, J. K.; Jung, Y. M. *J. Phys. Chem. B* **2006**, *110*, 23123.
- (18) Ryu, D. Y.; Lee, D. J.; Kim, J. K.; Lavery, K. A.; Russell, T. P.; Han, Y. S.; Seong, B. S.; Lee, C. H.; Thiagarajan, P. *Phys. Rev. Lett.* **2003**, *90*, 235501.
- (19) Ruzette, A.-V. G.; Mayes, A. M.; Pollard, M.; Russell, T. P.; Hammouda, B. *Macromolecules* **2003**, *36*, 3351.
- (20) Pollard, M.; Russell, T. P.; Ruzette, A.-V.; Mayes, A. M.; Gallot, Y. *Macromolecules* **1998**, *31*, 6493.
- (21) Varshney, S. K.; Hautekeer, J. P.; Fayt, R.; Jerome, R.; Teyssie, Ph. *Macromolecules* **1990**, *23*, 2618.
- (22) Balsara, N. P.; Perahia, D.; Safinya, C. R.; Tirrell, M.; Lodge, T. P. *Macromolecules* **1992**, *25*, 3896.
- (23) Bolze, J.; Kim, J.; Huang, J.; Rah, S.; Youn, H. S.; Lee, B.; Shin, T. J.; Ree, M. *Macromol. Res.* **2002**, *10*, 2.
- (24) Cho, J.; Sanchez, I. C. *Macromolecules* **1998**, *31*, 6650.
- (25) Cho, J. *Macromolecules* **2000**, *33*, 2228.
- (26) Cho, J. *Macromolecules* **2004**, *37*, 10101.
- (27) Cho, J. *J. Chem. Phys.* **2004**, *120*, 9831.
- (28) Cho, J. *Polymer* **2007**, *48*, 429.
- (29) Dudowicz, J.; Freed, K. F. *Macromolecules* **1991**, *24*, 5076.
- (30) Dudowicz, J.; Freed, K. F. *Macromolecules* **1993**, *26*, 213.
- (31) Dudowicz, J.; Freed, K. F. *Macromolecules* **2000**, *33*, 5292.
- (32) Freed, K. F.; Dudowicz, J. *Adv. Polym. Sci.* **2005**, *183*, 63.